



Citation for published version:

Wang, X, Wang, H & Xie, M 2020, 'Secret underneath: Fouling of membrane support layer in anaerobic osmotic membrane bioreactor (AnOMBR)', *Journal of Membrane Science*, vol. 614, 118530.
<https://doi.org/10.1016/j.memsci.2020.118530>

DOI:

[10.1016/j.memsci.2020.118530](https://doi.org/10.1016/j.memsci.2020.118530)

Publication date:

2020

Document Version

Peer reviewed version

[Link to publication](#)

Publisher Rights

CC BY-NC-ND

University of Bath

Alternative formats

If you require this document in an alternative format, please contact:
openaccess@bath.ac.uk

General rights

Copyright and moral rights for the publications made accessible in the public portal are retained by the authors and/or other copyright owners and it is a condition of accessing publications that users recognise and abide by the legal requirements associated with these rights.

Take down policy

If you believe that this document breaches copyright please contact us providing details, and we will remove access to the work immediately and investigate your claim.

1 **Secret underneath: fouling of membrane support layer in anaerobic osmotic membrane**
2 **bioreactor (AnOMBR)**

3

4

5 Xinhua Wang ^{a,*}, Hailong Wang ^a, Ming Xie ^{b,*}

6

7 **Journal of Membrane Science**

8 Revised: 9th July, 2020

9

10

11

12

13 ^a Jiangsu Key Laboratory of Anaerobic Biotechnology, School of Environmental and Civil
14 Engineering, Jiangnan University, Wuxi 214122, P.R. China

15

16 ^b Department of Chemical Engineering, University of Bath, Bath, BA2 7AY, UK

17

18

19

20 *Corresponding author. E-mail: xhwang@jiangnan.edu.cn (X. Wang), m.xie2@bath.ac.uk (M.
21 Xie); Tel: +86-510-85326516.

22 **Abstract**

23 Anaerobic osmotic membrane bioreactor (AnOMBR) holds promise for simultaneous
24 wastewater purification and biogas production, allowing for an energy and carbon-neutral
25 treatment facility. In a typical AnOMBR, reverse osmosis (RO) is employed for re-
26 concentrating draw solution for continuous operation and cost saving. We compared membrane
27 fouling behaviors between AnOMBR-RO hybrid system and AnOMBR without RO unit. We
28 concluded that the porous support layer was susceptible to both inorganic scaling and biofouling,
29 in the closed-loop AnOMBR-RO system. We also explored two cleaning approaches to mitigate
30 inorganic scaling and biofouling. Specifically, ethylenediaminetetraacetic acid (EDTA) was
31 introduced into draw solution for minimizing inorganic scaling, but biofouling was deteriorated
32 as EDTA provided extra nutrients for bacterial proliferation and biofouling. On the other hand,
33 chemical cleaning of membrane support layer was performed using NaClO solution for
34 biofouling control, but such cleaning efficacy attenuated after several cleaning cycles, because
35 inorganic minerals accumulated and grew within membrane porous layer which could not be
36 flushed by NaClO cleaning. Our finding highlighted the complexity and counter intuitive
37 perspective to membrane fouling and cleaning in AnOMBR-RO hybrid system for inorganic
38 scaling and biofouling management.

39

40 **Keywords:** membrane fouling, biofouling, support layer, forward osmosis, osmotic membrane
41 bioreactor, wastewater treatment

42 **1. Introduction**

43 With urbanization and industrial advancement of modern society, water shortage has
44 become a serious problem. In response to this water crisis and fulfilling United Nation
45 Sustainable Development Goal of ensuring availability and sustainable management of water
46 and sanitation for all, novel and high efficiency wastewater treatment technologies are required
47 to purify and recycle water sources. Forward osmosis (FO) is one such promising technology
48 that can bridge the gap in wastewater treatment and reuse. Previous studies demonstrated that
49 fouling trend of FO membrane was less severe compared to the pressure-driven membrane
50 processes [1-4].

51 Coupling FO process with biological treatment give birth to the development of anaerobic
52 membrane bioreactor (AnOMBR) that possesses superiority in water quality and bioresource
53 reclamation, as organic matters can be recovered in the form of biogas while nutrients such as
54 nitrogen, phosphorus in the form of struvite precipitation [5, 6]. However, severe membrane
55 fouling hinders the sustainable operation and deployment of AnOMBR as water flux decreased
56 sharply; and at the same time, the effluent quality was compromised. In an early effort, Chen et
57 al. [7] replaced traditional microfiltration (MF) membrane and ultrafiltration (UF) membrane
58 in AnOMBR by FO membrane, with the aim of obtaining high quality water and reducing
59 energy cost. Satisfactory phosphate (100%) and organic (>96.7%) removal were achieved by
60 FO membrane for municipal wastewater treatment. However, periodical supernatant
61 replacement was required for the feed side as the conductivity increased to 22 mS/cm, driven
62 by reverse solute diffusion from the draw side. In addition, severe membrane fouling hindered
63 the long-term, stable operation of the AnOMBR. For instance, Wang et al. [8] identified

64 membrane fouling in the active layer of FO membrane after 101-day AnOMBR operation. They
65 found that biofoulants, especially polysaccharides, proteins and microorganisms, were firmly
66 attached on membrane surface, thereby reducing water flux and shortening operation time.

67 Counter-intuitively, membrane fouling in AnOMBR can also occur within the membrane
68 support layer, particularly in a closed-loop system. For instance, significant fouling within
69 membrane support layer was reported by Kim et al. [9], and membrane physical flushing proved
70 futile as foulants occurred and trapped inside the porous cellulose triacetate support layer. Such
71 detrimental membrane fouling was driven by the contaminant accumulation within draw
72 solution in a closed-loop system where draw solution was re-concentrated through a wide range
73 of separation processes, such as, nano-filtration (NF) [10], membrane distillation (MD) [11]
74 and reverse osmosis (RO) [12]. For instance, when treating digested sludge feed by an FO-RO
75 membrane system, Xie et al. [13] found that protein-like substance was the major constituent
76 that accumulated in the draw solution, which could pass through FO membrane while be
77 rejected by RO membrane. In addition, Choi et al. [14] also reported that membrane fouling
78 shifted from RO membrane to FO membrane in treatment of secondary wastewater effluent in
79 the FO-RO hybrid system, confirming the transportation of low molecule weight substance to
80 the DS side. In their long-term, pilot-scale FO-RO osmotic dilution process to treat wastewater
81 from coal-fired power station [15], they observed contaminants accumulation in the draw
82 solution which was detrimental to downstream RO membrane. As a result, in a closed-loop
83 AnOMBR, there exists an unavoidable issue associated with contaminant buildup in the draw
84 solution; and consequently, membrane fouling in the support layer of the AnOMBR system was
85 hypothesized due to constant accumulation of inorganic and organic compounds in draw

86 solution.

87 In this study, we investigated membrane fouling in a closed-loop AnOMBR system,
88 coupling with the RO unit to re-concentrate draw solution. Filtration performance and fouling
89 behavior of AnOMBR-RO hybrid system were examined and analyzed. Varying approaches for
90 membrane cleaning were performed and compared to alleviate membrane fouling within the
91 membrane support layer (i.e., the side facing draw solution). Findings reported here shed
92 insights into membrane fouling mechanisms in the AnOMBR-RO hybrid system, and offered
93 effective membrane fouling mitigation strategies for sustainable AnOMBR operation.

94

95 **2. Materials and methods**

96 2.1 Bioreactor set-up and operating conditions

97 Details of the AnOMBR were reported in our previous literatures [8, 16]. Briefly, the
98 effective volume of the AnOMBR unit was 5 L; two pieces of cellulose triacetate (CTA)
99 membrane (provided by Hydration Technologies Inc.) with the total area of 0.025 m² were
100 placed in the FO module; the FO module as well as an MF membrane with the identical
101 membrane area were immersed in the bioreactor. 0.5 M NaCl was used as draw solution during
102 the operation and its concentration was maintained in the comparatively stable level by the
103 conductivity controller (OKD-650, Shenzhen OK Instrument Technology, China) connected to
104 the concentrated NaCl solution of 5 M. Permeate water flux of the MF membrane was adjusted
105 to achieve the low salinity environment in the feed side and the conductivity of the mixed sludge
106 was controlled around 2-4 mS/cm.

107 An RO unit (STM-0021-HP, Starmen Scitechnology, Xia'men, China) was used to
108 concentrate draw solution for AnOMBR. The RO unit was operated in batch mode with SW30

109 RO membrane (Dow, Filmtec) with well documented NaCl rejection above 99.4%: when the
110 draw solution volume reached 1.3 times of its initial volume, RO was operated at 4 MPa until
111 the draw solution had been concentrated to its initial volume. The start and stop of RO unit
112 were automatically controlled through water level sensor. The draw solution temperature was
113 maintained as $25 \pm 1^\circ\text{C}$.

114 Two AnOMBR systems were used for fair comparison of membrane fouling: AnOMBR
115 was operated with draw solution being discarded, which was denoted as R1; the
116 AnOMBR hybrid with RO was denoted as R2. Specifically, synthetic municipal
117 wastewater was used as influent and its composition can be found in previous literatures
118 [8, 15]. The initial mixed liquor suspended solids (MLSS) concentration was 2.8 g/L
119 and the MLVSS/MLSS value was 0.6 at the beginning. This selection of initial MLSS
120 was reflected as a low strength feed wastewater, and was consistent with ample previous
121 literatures [7, 8, 16-19].

122 During the operation, the sludge retention time (SRT) was set as 100 days while
123 the hydraulic retention time was decided by the FO and MF permeate fluxes.

124 Membrane fouling mitigation was carried out via two approaches: introducing
125 ethylenediaminetetraacetic acid (EDTA) into draw solution or performing chemical cleaning
126 by NaClO solution. Specifically, 20 mg/L EDTA was added into 0.5 M NaCl draw solution in
127 AnOMBR-RO hybrid system, which was denoted as R3. Periodical chemical cleaning was
128 performed every five days. During NaClO cleaning, 2 L NaClO solution (50 mg/L) was
129 circulated in the module through a peristaltic pump for 15 min followed by DI water rising for
130 15 min. The AnOMBR-RO hybrid system with periodical chemical cleaning was denoted as
131 R4.

132 2.2 Analytical methods

133 Influent, effluent and sludge supernatant samples were analyzed for $\text{NH}_4^+\text{-N}$, total nitrogen
134 (TN) and total phosphorus (TP) concentrations using standard method. TOC analyzer (TOC-

135 V_{CPH} , Shimadzu, Japan) was used to measure the TOC concentrations by combustion oxidation
136 method. Inductively coupled plasma optical emission spectrometer (ICP-OES, Optima 8300,
137 PerkinElmer, USA) was used to analyze ion profile of draw solution samples at the conclusion
138 of each batch operation. Concentration in the draw solution was corrected by taking
139 concentration factor into account due to the batch mode operation in RO unit. The corrected
140 concentration was then used for calculation of the removal efficiency of the whole AnOMBR
141 system. Morphology observation of the fouled membranes was carried out by a HITACHI
142 S3400 scanning electron microscope (SEM).

143 In order to analyze the membrane biofouling, membrane samples were stained by
144 Concanavalin A (ConA), Calcofluor white (CW), Fluorescein isothiocyanate (FITC) and
145 SYTO™ 63 in order to analyze the spatial distribution of α -D-glucopyranose and β -D-
146 glucopyranose polysaccharides, proteins and microorganisms, with a confocal laser scanning
147 microscope (CLSM, TCS SP8, Leica, Germany). Detailed information about sample
148 preparation and data calculation can be found in our previous publications [20, 21]. Briefly, the
149 fouled FO membranes were taken out from the bioreactor at the conclusion of the
150 operation; and then three pieces with size of about 1×1 cm were randomly cut from
151 each fouled FO membrane. The fouled membrane samples were first stained with
152 SYTO 63 ($20 \mu\text{M}$), and then the FITC solution (10 g L^{-1}) was dripped onto the samples
153 after 1 M sodium bicarbonate (NaHCO_3) buffer was applied for keeping the amine
154 group in a non-protonated form. Subsequently, the ConA (0.25 g L^{-1}) and CW (0.3 g L^{-1})
155 solutions were added to the samples, respectively. After each stage of the labelling
156 process, the samples were incubated for 30 min at room temperature in the dark, and

157 then were washed twice with phosphate buffered saline (PBS) solution to remove the
158 extra probes. The three-dimensional reconstructions were obtained with ZEISS confocal
159 software, and the images were analyzed by PHLIP and Image J to calculate the quantitative
160 parameters, including biovolume, and average biofouling thickness.

161 For cleaning and analyzing inorganic scaling of the fouled membrane, 0.5% hydrochloric
162 (HCl) as well as 0.5% hydrogen peroxide (H₂O₂) was used to rinse the membrane support layers,
163 respectively, to remove inorganic and organic contaminants [16]. After that, membrane samples
164 were cut into 1 cm × 1 cm, and were dried in the oven at 60 °C for 12 h. Dried samples were
165 heated to 600°C in the furnace for two hours, the weight loss before and after calcination
166 represented organic compounds, and the main components of the residue were inorganic scale.

167 **3. Results and discussion**

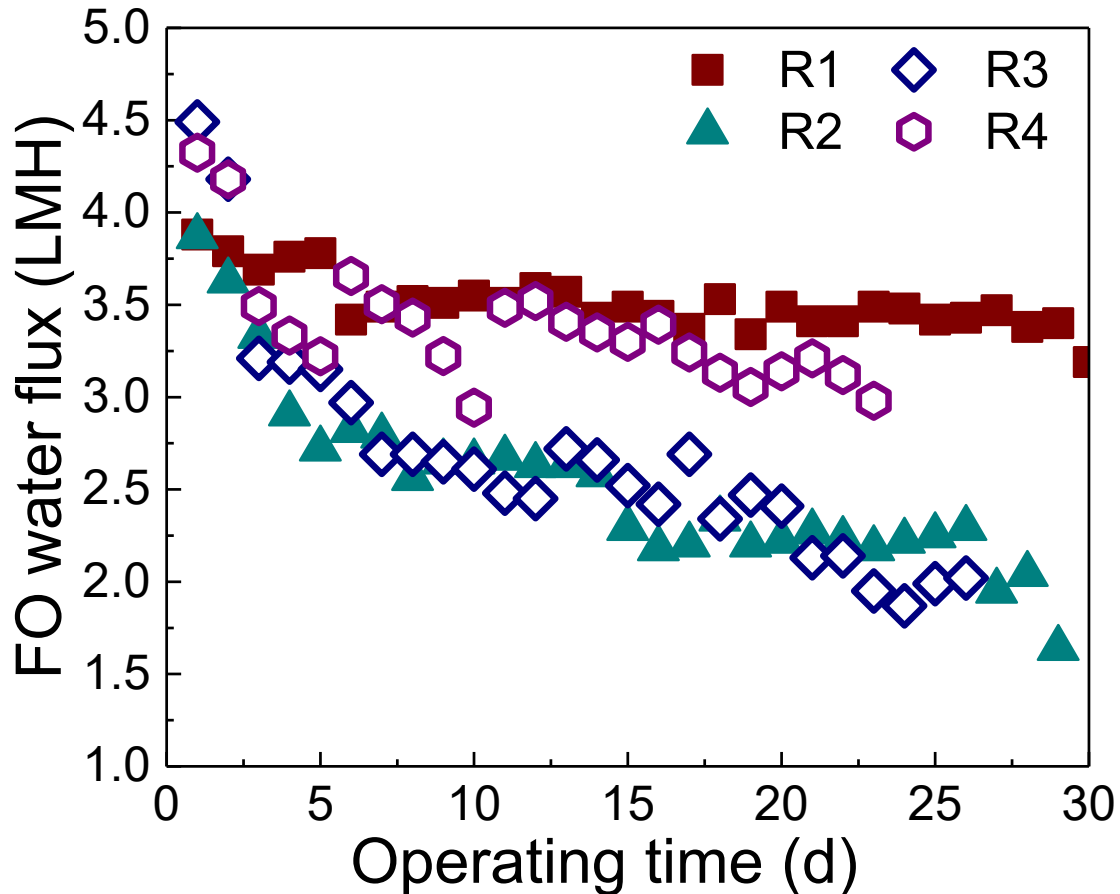
168 **3.1 Bioreactor performance: contaminant removal and water production**

169 Stable operating performance was achieved in both R1 and R2 reactors (Figure 1). Owing
170 to the addition of MF membrane, salinity of the two bioreactors was well controlled between 2
171 and 5 mS/cm during operations, which was one order of magnitude lower than a typical
172 AnOMBR [7]. It further corroborated that OMBR coupled with MF membrane could obtain
173 long-term operation under lower salinity environment. Effluent of higher quality was produced
174 from R2 due to the dual membrane barrier.

175 Both bioreactors achieved high product water quality. Nearly no phosphorus was detected
176 in the RO permeate of R2 (Figure S3). In R2, noticeable ammonia nitrogen (up to 59 mg/L)
177 accumulated in the draw solution and was due to Donnan effect [22, 23]. This phenomena
178 was mainly attributed to bidirectional diffusion of ammonium of feed solution and

179 sodium cations of draw solution in forward osmosis process; and on the other hand,
180 ammonia nitrogen was relatively well rejected by RO unit, thereby resulting in the final
181 concentration of ammonia nitrogen in the product water from R2 lower than 8.8 mg/L
182 (Figure S4). For organic removal in R2, the TOC concentration in RO permeate was 4% lower
183 than that in FO permeate. It was mainly driven by the similar solute-rejecting capacity for FO
184 and RO membrane used in the experiment whose molecular weight cutoffs were 250 Da and
185 180 Da, respectively [14]. Amino acids as well as proteins with low molecule weight could
186 easily pass through both FO and RO membranes.

187 In addition, as AnOMBR featured in biogas production during anaerobic process, the
188 methane yield ranged from 0.25 to 0.30 L CH₄/g COD in both R1 and R2 reactors, which was
189 consistent with previous data on AnOMBR [7, 8, 16].



190

191 **Figure 1:** FO permeate flux for different bioreactors as a function of operating time. R1:
192 AnOMBR without RO unit; R2: AnOMBR hybrid system with RO unit; R3: AnOMBR hybrid
193 system with RO unit, and EDTA was added to the draw solution; R4: AnOMBR hybrid with
194 RO unit, and periodically NaClO chemical cleaning was performed every 5 days.

195

196 Water fluxes in both R1 and R2 were stable during the operation, although CTA FO
197 membranes used in AnOMBR possessed relatively low water flux. Indeed, water flux of FO
198 membrane in R1 was 3.5 LMH in average during the 30-day operation (solid square in Figure
199 1) and was similar to Wang et al. [8] whose water flux ranged from 2.5 to 3.5 LMH during the
200 stable stage. However, water flux for CTA FO membrane in R2 hybrid system decreased sharply
201 and the stable water flux was around 2 LMH (solid triangle in Figure 1), which was 42% less
202 in water production. The key difference between R1 and R2 was the addition of downstream
203 RO unit for a closed-loop system. It was hypothesized that such significant discrepancy in water
204 flux profile was mainly driven by membrane fouling. Particularly, bio-fouling and inorganic
205 scaling were substantially different for these two bioreactors as membrane fouling occurred not
206 only in the membrane active layer but also in the membrane support layer in the closed-loop
207 bioreactor as R2. In another word, the biofouling occurred on the membrane active layer was
208 not the key reason for water flux deterioration, but the biofouling and scaling developed within
209 the membrane porous support layer that dictated the system performance.

210

211 **3.2 Membrane fouling in AnOMBR**

212 3.2.1 Membrane fouling in membrane active layer revealed negligible difference

213 Key characteristics of biofouling layer in two AnOMBRs (R1 and R2) were imaged and
214 compared (Figure S6). In generally, the biofouling on membrane active layers were similar for

215 R1 and R2 in terms of biofouling layer thickness and biovolume. There were negligible
216 difference in composition of biofouling layer for either AnOMBR (R1 and R2). Specifically,
217 the total thickness of biofouling layer was $61.40 \pm 3.84 \mu\text{m}$ and $61.40 \pm 1.54 \mu\text{m}$ for R1 and R2,
218 respectively. In addition, average thickness of β -D-glucopyranose polysaccharides and proteins
219 was $32.01 \pm 0.05 \mu\text{m}$ and $37.89 \pm 3.97 \mu\text{m}$ for R1; and was $26.44 \pm 3.65 \mu\text{m}$ and 31.16 ± 3.69
220 μm for R2, respectively. Moreover, similar inorganic composition of the fouling layer on the
221 membrane active layer was observed. Weight percentage of inorganic mineral accounted for
222 5.6% and 6.1% for R1 and R2, respectively. As a result, it was concluded that membrane fouling
223 in membrane active layer was similar in both bioreactors, and cannot sufficiently explain the
224 discrepancy in system performance.

225

226 3.2.2 Membrane fouling in membrane support layer was critical and substantially different

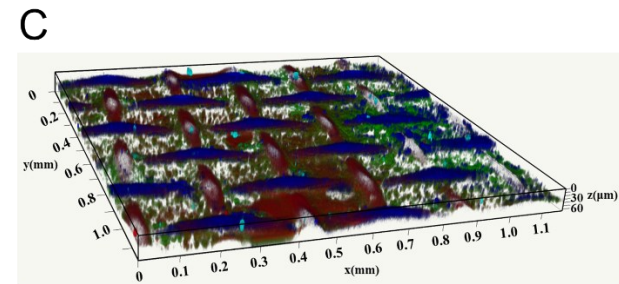
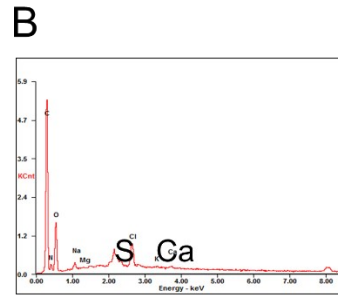
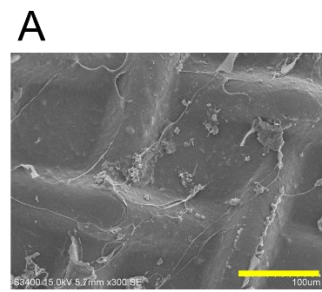
227 Biofouling and inorganic scaling within membrane support layer were systematically
228 analyzed and compared in different AnOMBRs (R1 and R2). Evidence for bacteria proliferation
229 and biofilm development within membrane support layer in both AnOMBR was highlighted in
230 element analysis where strong peak of sulfur (Figure 2E) existed due to bacterial metabolism.
231 Indeed, CLSM images of the membrane support layers illustrated the occurrence of biofouling
232 (Figures 2 C and F). More importantly, biofouling in R2 AnOMBR was more severe than that
233 in R1 one. The thickness of the fouling layers of R1 and R2 were similar of $61.68 \pm 1.92 \mu\text{m}$
234 and $57.33 \pm 0.38 \mu\text{m}$, respectively. In addition, biovolume of biofilm was quantified and
235 summarized in Table 1. For R2 AnOMBR, volumes of β -D-glucopyranose, proteins and total
236 cells were 111.04%, 53.96% and 16.61% higher than that for R1, respectively, indicating active

237 biofilm growth and severe biofouling.

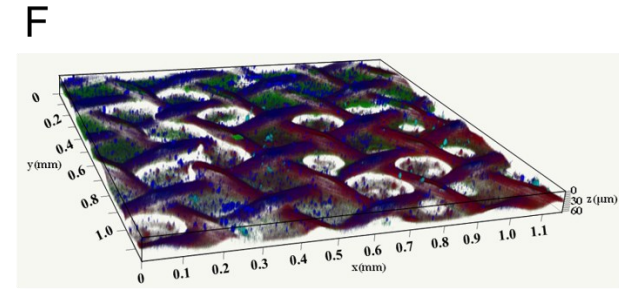
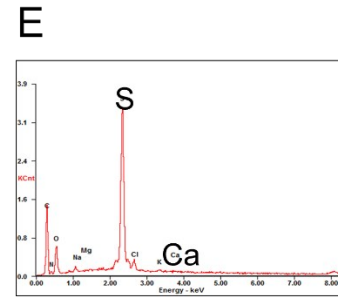
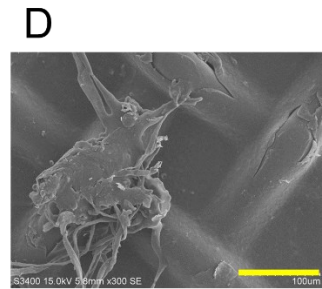
238 Such unfavorable biofouling in closed-loop R2 AnOMBR was mainly driven by the
239 accumulation of nutrients and low molecule-weight organic substance in the draw solution [10,
240 11, 14]. Bacteria would utilize the accumulated nutrients in the draw solution, thereby excreting
241 metabolites such as, extracellular polymeric substances and varying proteins would facilitate
242 biofilm growth within membrane support layer [24], resulting in severe biofouling.

243 From the perspective of inorganic scaling, ion profile of draw solution for both AnOMBR
244 raised concern for inorganic scaling, particularly for mineral precipitation of CaCO_3 and
245 MgCO_3 within the membrane porous support layer. Indeed, concentrations of calcium and
246 magnesium ions in the draw solution for AnOMBR-RO hybrid system (R2) were an order of
247 magnitude higher than those for AnOMBR (R1) (Table S1). Given that the solubility product
248 constant (K_{sp}) of CaCO_3 and MgCO_3 were $10^{-8.48}$ and $10^{-5.17}$, respectively [25, 26], it is highly
249 likely that CaCO_3 precipitation could occur and could subsequently deposit within the porous
250 support layer, thereby deteriorating internal concentration polarization and decreasing FO
251 permeate water flux [27]. As a result, it was necessary to inhibit the formation of calcium
252 carbonate via either pH adjustment or adding scale inhibitors.

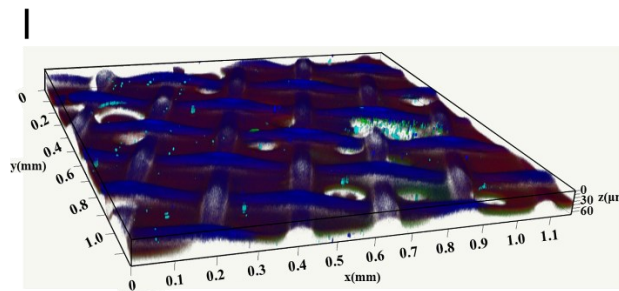
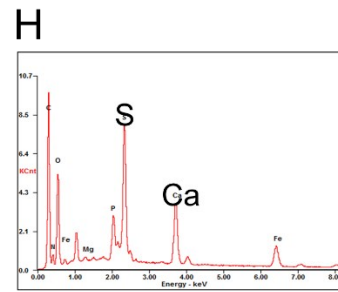
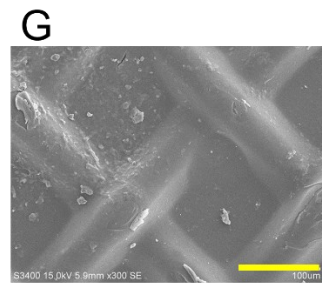
AnOMBR, **R1**



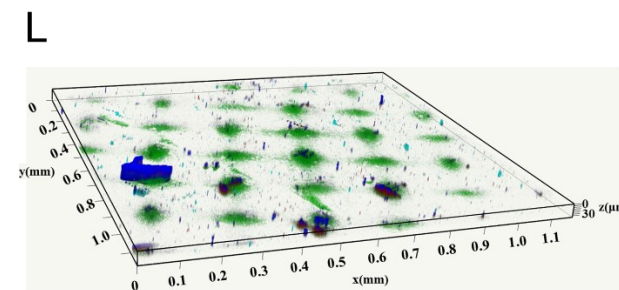
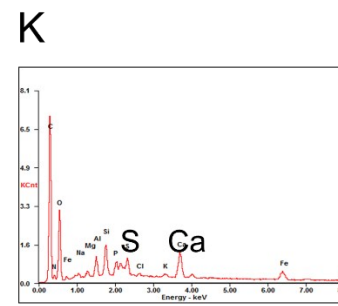
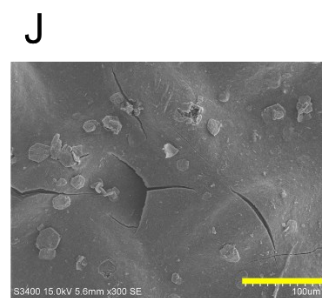
AnOMBR
with
RO unit, **R2**



AnOMBR
with
RO unit;
EDTA draw,
R3



AnOMBR with
RO unit;
NaClO cleaning,
R4



254 **Figure 2:** Characterisation of membrane fouling of membrane porous support layer in four
255 different AnOMBRs (A-C for AnOMBR, R1; D-F for AnOMBR hybrid with the RO unit, R2;
256 G-I for AnOMBR hybrid with the RO unit, and EDTA was added to the draw solution, R3; and
257 J-L for AnOMBR hybrid with the RO unit, and periodically NaClO cleaning was performed
258 every 5 days, R4). SEM and EDX element analysis of fouled porous membrane support layer
259 for (A and B) R1, (D and E) R2, (G and H) R3 and (J and K) R4. Scale bar in the scanning
260 electron microscope is 100 μm . CLSM 3D images of fouled porous membrane support layer
261 for (C) R1, (F) R2, (I) R3 and (L) R4.

262

263 3.3 Fouling mitigation in membrane support layer of AnOMBR

264 3.3.1 Introducing EDTA into draw solution

265 Introducing chelate reagent into draw solution can be an effective approach to mitigate
266 inorganic scaling, particularly CaCO_3 . In R3, EDTA was introduced into the draw solution to
267 minimize CaCO_3 scaling within membrane porous support layer. EDTA, with a relatively large
268 molecular weight, could be well rejected by the FO and RO membrane, which corroborated by
269 similar TOC concentration in the final product water from R2 (6.75 mg/L) and R3 (6.61 mg/L)
270 (Figure S2).

271 Unexpectedly, FO water flux profiles in R2 and R3 were similar after introducing EDTA
272 into draw solution (Figure 1). Such counter-intuitive phenomena raised concern why EDTA had
273 an adverse effect on flux performance while it could work effectively as scale inhibitor. It was
274 hypothesized that addition of EDTA into draw solution could introduce carbon and nitrogen
275 source that were favorable for microorganism activities. **Indeed, EDTA may be used as a carbon**
276 **source and a nitrogen source in bacterial growth [28]. In addition, EDTA is also an effective**
277 **ligand to most cations, thereby being helpful for the uptake of essential elements to facilitate**
278 **biofilm development.** Strong peaks of nitrogen and sulfur were detected on the membrane
279 support layer from AnOMBR R3 (Figure 2H), which indicated active biofilm development.

280 More alarming, the CLSM images of membrane support layer from AnOMBR R3 demonstrated
281 a thick and compact biofouling layer (Figure 2I). In addition, detailed analysis of biovolume
282 composition of biofouling in AnOMBR R3 (Table 1) demonstrated that biovolume of β -D-
283 glucopyranose polysaccharides, proteins and total cells in R3 were 37%, 35 % and 43% higher
284 than those in R2.

285 **Table 1:** Comparison of biofilm characteristics in the membrane support layers in different AnOMBRs ^a

286

AnOMBR	Thickness (μm)	α -D-glucopyranose ($\mu\text{m}^3/\mu\text{m}^2$)	β -D-glucopyranose ($\mu\text{m}^3/\mu\text{m}^2$)	Proteins ($\mu\text{m}^3/\mu\text{m}^2$)	Total cells ($\mu\text{m}^3/\mu\text{m}^2$)
R1	61.68 \pm 1.92	4.06 \pm 0.23	4.44 \pm 0.64	5.30 \pm 1.14	6.44 \pm 0.04
R2	57.33 \pm 0.38	4.04 \pm 0.01	9.37 \pm 1.41	8.16 \pm 0.58	7.51 \pm 0.47
R3	63.15 \pm 0.64	4.65 \pm 2.13	12.81 \pm 0.91	11.04 \pm 1.16	10.71 \pm 3.90
R4	32.71 \pm 0.26	4.42 \pm 0.29	6.43 \pm 0.35	9.90 \pm 1.17	5.89 \pm 1.36

287 ^a Values are presented as average values \pm standard deviation (number of measurements: n = 3 from two random samples).

288 3.3.2 Periodical, chemical cleaning of membrane support layer

289 Another perspective to control membrane fouling within support layer in AnOMBR was
290 periodical chemical cleaning using NaClO. NaClO solution can oxidize microorganisms as well
291 as part of biofoulants, which is extensively used in MBR cleaning [29]. Indeed, 1% NaClO
292 cleaning was used by Linares et al. [30] for CTA FO membrane in a sequential batch reactor-
293 FO system, and achieved satisfying water flux recovery.

294 Periodical, NaClO chemical cleaning was performed every five days in AnOMBR R4.
295 Such NaClO chemical cleaning was effective in membrane biofouling control and water flux
296 recovery. Biofilm establishment and growth were strongly inhibited with NaClO cleaning. Only
297 patchy biofilm could be visualized on the membrane support layer using CLSM (Figure 2I).
298 Coincidentally, biovolume of β -D-glucopyranose polysaccharides and total cells were
299 substantially reduced in R4 AnOMBR, being only 68% and 78% of those in AnOMBR R2
300 (Table 1).

301 Such chemical cleaning not only effectively mitigate membrane biofouling, but also
302 enhanced FO water flux recovery. R4 AnOMBR demonstrated higher stable water flux in
303 comparison to both R2 and R3 AnOMBRs. Distinctively, FO water flux was promptly restored
304 after NaClO chemical cleaning at day 10 (Figure 1). However, efficacy of NaClO chemical
305 cleaning attenuated at days 16 and 21, achieving only 4.2% and 2.2% water flux recovery,
306 respectively. This diminishing cleaning performance was due to the accumulation of inorganic
307 scalants that were trapped within membrane support layer and could not be washed by NaClO
308 chemical cleaning. Indeed, SEM imaging and element analysis confirmed that inorganic
309 crystals, particularly calcium-based scalants, filled in the membrane porous support layer

310 (Figure 2K).

311

312 **4. Conclusion**

313 Results reported here showed that closed-loop AnOMBR-RO system experienced more
314 severe fouling than single AnOMBR. This discrepancy in AnOMBR performance cannot be
315 explained by similar membrane biofouling on the membrane active layer. Severe fouling
316 occurred within the membrane support layer in the AnOMBR-RO hybrid system, featuring
317 inorganic fouling and biofouling. A set of two approaches – introducing EDTA into draw
318 solution and NaClO chemical cleaning – were carried out to mitigate the membrane fouling
319 within membrane support layer in the AnOMBR. Results showed that EDTA could work as
320 inhibitor to cope with inorganic scalant precipitation; but it could provide nutrients for microbes,
321 which would deteriorate biofouling conversely. On the other hand, periodical NaClO chemical
322 cleaning could effectively control biofouling, but while such efficacy attenuated after several
323 cleaning cycles due to calcium-based inorganic crystals accumulated within the porous support
324 layer.

325 Implications gleaned from this study shed light on membrane fouling mechanisms and
326 cleaning approaches for AnOMBR application. Such counter-intuitive findings shifted focus to
327 membrane fouling within porous membrane support layer in the closed-loop bioreactors. In
328 addition, there was a trade-off in controlling biofouling and inorganic scaling in the AnOMBR
329 operation, which demands a holistic approach to mitigate membrane fouling for sustainable
330 AnOMBR operation.

331

332 **5. Acknowledgements**

333 This work was supported by Grants from the National Natural Science Foundation of
334 China (grant number 51978312); the Six Major Talent Peaks of Jiangsu Province (grant number
335 2018-JNHB-014); and Jiangsu Cooperative Innovation Center of Technology and Material of
336 Water Treatment.

337

338 **6. References**

339

340 [1] A. Achilli, T.Y. Cath, E.A. Marchand, A.E. Childress, The forward osmosis membrane bioreactor: a low
341 fouling alternative to MBR processes, *Desalination*, 239 (2009) 10-21.

342 [2] T.Y. Cath, M. Elimelech, J.R. McCutcheon, R.L. McGinnis, A. Achilli, D. Anastasio, A.R. Brady, A.E.
343 Childress, I.V. Farr, N.T. Hancock, Standard methodology for evaluating membrane performance in
344 osmotically driven membrane processes, *Desalination*, 312 (2013) 31-38.

345 [3] D.L. Shaffer, J.R. Werber, H. Jaramillo, S. Lin, M. Elimelech, Forward osmosis: where are we now?,
346 *Desalination*, 356 (2015) 271-284.

347 [4] X. Wang, V.W. Chang, C.Y. Tang, Osmotic membrane bioreactor (OMBR) technology for wastewater
348 treatment and reclamation: Advances, challenges, and prospects for the future, *Journal of membrane
349 science*, 504 (2016) 113-132.

350 [5] M. Zuthi, H. Ngo, W. Guo, Modelling bioprocesses and membrane fouling in membrane bioreactor
351 (MBR): a review towards finding an integrated model framework, *Bioresour. Technol.*, 122 (2012) 119-
352 129.

353 [6] P. Krzeminski, L. Leverette, S. Malamis, E. Katsou, Membrane bioreactors—a review on recent
354 developments in energy reduction, fouling control, novel configurations, LCA and market prospects,
355 *Journal of Membrane Science*, 527 (2017) 207-227.

356 [7] L. Chen, Y. Gu, C. Cao, J. Zhang, J.-W. Ng, C. Tang, Performance of a submerged anaerobic membrane
357 bioreactor with forward osmosis membrane for low-strength wastewater treatment, *Water Research*,
358 50 (2014) 114-123.

359 [8] X. Wang, C. Wang, C.Y. Tang, T. Hu, X. Li, Y. Ren, Development of a novel anaerobic membrane
360 bioreactor simultaneously integrating microfiltration and forward osmosis membranes for low-strength
361 wastewater treatment, *Journal of Membrane Science*, 527 (2017) 1-7.

362 [9] Y. Kim, S. Li, L. Chekli, Y.C. Woo, C.-H. Wei, S. Phuntsho, N. Ghaffour, T. Leiknes, H.K. Shon, Assessing
363 the removal of organic micro-pollutants from anaerobic membrane bioreactor effluent by fertilizer-
364 drawn forward osmosis, *Journal of Membrane Science*, 533 (2017) 84-95.

365 [10] C. Tan, H. Ng, A novel hybrid forward osmosis-nanofiltration (FO-NF) process for seawater
366 desalination: Draw solution selection and system configuration, *Desalination and water treatment*, 13
367 (2010) 356-361.

368 [11] M. Xie, L.D. Nghiem, W.E. Price, M. Elimelech, A forward osmosis–membrane distillation hybrid
369 process for direct sewer mining: system performance and limitations, *Environmental science &*

370 technology, 47 (2013) 13486-13493.

371 [12] O. Bamaga, A. Yokochi, B. Zabara, A. Babaqi, Hybrid FO/RO desalination system: Preliminary
372 assessment of osmotic energy recovery and designs of new FO membrane module configurations,
373 Desalination, 268 (2011) 163-169.

374 [13] M. Xie, S.R. Gray, Transport and accumulation of organic matter in forward osmosis-reverse osmosis
375 hybrid system: Mechanism and implications, Sep. Purif. Technol., 167 (2016) 6-16.

376 [14] B.G. Choi, D.I. Kim, S. Hong, Fouling evaluation and mechanisms in a FO-RO hybrid process for direct
377 potable reuse, Journal of Membrane Science, 520 (2016) 89-98.

378 [15] B.G. Choi, M. Zhan, K. Shin, S. Lee, S. Hong, Pilot-scale evaluation of FO-RO osmotic dilution process
379 for treating wastewater from coal-fired power plant integrated with seawater desalination, Journal of
380 Membrane Science, 540 (2017) 78-87.

381 [16] X. Wang, T. Hu, Z. Wang, X. Li, Y. Ren, Permeability recovery of fouled forward osmosis membranes
382 by chemical cleaning during a long-term operation of anaerobic osmotic membrane bioreactors treating
383 low-strength wastewater, Water Research, 123 (2017) 505-512.

384 [17] Y. Gu, L. Chen, J.-W. Ng, C. Lee, V.W.C. Chang, C.Y. Tang, Development of anaerobic osmotic
385 membrane bioreactor for low-strength wastewater treatment at mesophilic condition, Journal of
386 Membrane Science, 490 (2015) 197-208.

387 [18] X. Wang, J. Zhang, V.W.C. Chang, Q. She, C.Y. Tang, Removal of cytostatic drugs from wastewater by
388 an anaerobic osmotic membrane bioreactor, Chemical Engineering Journal, 339 (2018) 153-161.

389 [19] H. Wang, X. Wang, F. Meng, X. Li, Y. Ren, Q. She, Effect of driving force on the performance of
390 anaerobic osmotic membrane bioreactors: New insight into enhancing water flux of FO membrane via
391 controlling driving force in a two-stage pattern, Journal of Membrane Science, 569 (2019) 41-47.

392 [20] B. Yuan, X. Wang, C. Tang, X. Li, G. Yu, In situ observation of the growth of biofouling layer in osmotic
393 membrane bioreactors by multiple fluorescence labeling and confocal laser scanning microscopy, Water
394 Res., 75 (2015) 188-200.

395 [21] L.N. Mueller, J.F. De Brouwer, J.S. Almeida, L.J. Stal, J.B. Xavier, Analysis of a marine phototrophic
396 biofilm by confocal laser scanning microscopy using the new image quantification software PHILIP, BMC
397 ecology, 6 (2006) 1.

398 [22] E.A. Bell, R.W. Holloway, T.Y. Cath, Evaluation of forward osmosis membrane performance and
399 fouling during long-term osmotic membrane bioreactor study, Journal of Membrane Science, 517 (2016)
400 1-13.

401 [23] X. Lu, C. Boo, J. Ma, M. Elimelech, Bidirectional Diffusion of Ammonium and Sodium Cations in
402 Forward Osmosis: Role of Membrane Active Layer Surface Chemistry and Charge, Environmental
403 Science & Technology, 48 (2014) 14369-14376.

404 [24] E. Bar-Zeev, F. Perreault, A.P. Straub, M. Elimelech, Impaired Performance of Pressure-Retarded
405 Osmosis due to Irreversible Biofouling, Environmental Science & Technology, 49 (2015) 13050-13058.

406 [25] A. Godelitsas, J.M. Astilleros, K. Hallam, S. Harissopoulos, A. Putnis, Interaction of calcium
407 carbonates with lead in aqueous solutions, Environmental science & technology, 37 (2003) 3351-3360.

408 [26] D.H. Case, F. Wang, D.E. Giammar, Precipitation of magnesium carbonates as a function of
409 temperature, solution composition, and presence of a silicate mineral substrate, Environmental
410 Engineering Science, 28 (2011) 881-889.

411 [27] Q. She, R. Wang, A.G. Fane, C.Y. Tang, Membrane fouling in osmotically driven membrane processes:
412 A review, Journal of Membrane Science, 499 (2016) 201-233.

413 [28] R.A.P. Thomas, K. Lawlor, M. Bailey, L.E. Macaskie, Biodegradation of Metal-EDTA Complexes by an

414 Enriched Microbial Population, *Applied and Environmental Microbiology*, 64 (1998) 1319.
415 [29] Z. Wang, J. Ma, C.Y. Tang, K. Kimura, Q. Wang, X. Han, Membrane cleaning in membrane bioreactors:
416 a review, *Journal of Membrane Science*, 468 (2014) 276-307.
417 [30] R.V. Linares, Z. Li, V. Yangali-Quintanilla, Q. Li, J.S. Vrouwenvelder, G.L. Amy, N. Ghaffour, Hybrid
418 SBR–FO system for wastewater treatment and reuse: Operation, fouling and cleaning, *Desalination*, 393
419 (2016) 31-38.
420